Engineering Structures 45 (2012) 472–480

Contents lists available at SciVerse ScienceDirect

Engineering Structures

journal homepage: www.elsevier.com/locate/engstruct

Comparing vector-valued intensity measures for fragility analysis of steel frames in the case of narrow-band ground motions

Edén Bojórquez [a,*], Iunio Iervolino [b], Alfredo Reyes-Salazar [a], Sonia E. Ruiz [c]

[a] Facultad de Ingeniería, Universidad Autónoma de Sinaloa, Calzada de las Américas y B. Universitarios s/n, C.P. 80040, Culiacán, Sinaloa, Mexico
[b] Dipartimento di Ingegneria Strutturale, Università degli Studi di Napoli Federico II, Via Claudio 21, 80125, Naples, Italy
[c] Instituto de Ingeniería, Universidad Nacional Autónoma de México, Apdo. Postal 70-472, Coyoacán, C.P. 04510, México, D.F., Mexico

ARTICLE INFO

Article history:
Received 14 November 2011
Revised 17 April 2012
Accepted 8 July 2012

Keywords:
Spectral shape
Maximum inter-story drift
Energy-based damage index

ABSTRACT

Seismic fragility of steel frames subjected to narrow-band motions from soft-soils of Mexico City (Mexico) is evaluated by means of a set of vector-valued ground motion intensity measures (*IMs*) comprised of two parameters. All the vectors considered have, as the first component, spectral acceleration at the first mode of the structure. As the second component, compared *IMs* are chosen among peak and integral parameters, the former represent the spectral shape in a range of periods, while the latter refer to cumulative damage potential of earthquakes. The maximum inter-story drift and an energy-based damage index for steel frames are employed as engineering demand parameters for structural performance assessment. As a result of the comparison, it is observed that spectral-shape-based vector-valued *IMs* have the best explicative power with respect to seismic fragility estimation. Analyses, even if limited to the peculiar ground motions considered, suggest that a recently proposed parameter (N_p) is especially promising as a candidate for the next generation of *IMs* when combined with spectral acceleration. This appears independent of the type of seismic response measure considered.

1. Introduction

Earthquake ground motion potential with respect to structural performance is usually characterized by a parameter named intensity measure (*IM*). In the context of performance-based earthquake engineering [1,2], the desirable features of an *IM* are: *efficiency*, which is the ability of the *IM* to predict the response of a structure subjected to earthquakes with comparatively small heterogeneity; *sufficiency*, which implies that given an *IM* value, the structural response is insensitive to other parameters, for example, magnitude and distance of the source; and scaling *robustness*, that is, unbiased estimation of structural demand when the records are linearly scaled to perform structural assessment at different earthquake intensity levels (e.g. [3]).

IMs, which represent the variables interfacing ground motion and structural response, have been the subject of a great deal of research since the origin of earthquake engineering [4–12]. In the past, parameters as peak ground acceleration (*PGA*), peak ground velocity (*PGV*), Arias Intensity (I_A) [5], among others, were commonly used as *IMs*. More recently, the elastic spectral acceleration at first mode of vibration of the structure, $Sa(T_1)$, has been thoroughly studied, especially because its efficiency in several cases of linear and non-linear structural response, and because most of the worldwide seismic hazard maps quantify the seismic threat in terms of probability of exceedance of this parameter. Moreover, studies have found the sufficiency of this *IM*, with respect to magnitude and distance, and robustness [7,13]. Nevertheless, some limitations of $Sa(T_1)$ have been observed recently, and for this reason different researchers promote the use of vector-valued *IMs* [9,14].

Vector-valued *IMs* are based on the use of two or more parameters with the aim of predicting the response of a structure with larger efficiency with respect to scalar measures (in principle, because more information about ground motion is included in the definition of its intensity), and/or to achieve sufficiency in those cases when scalar *IMs* do not warrant it (e.g., [15]). Currently, the most relevant scalar and vector-valued *IMs* for structural seismic risk assessment appear to be those which try to capture the elastic response spectrum shape in a range of oscillation periods (e.g., [12,16]). In fact, the critical success factor in the definition of vector-valued intensity measures comprised of two parameters is to obtain the pair with the best explicative power with respect to structural response. Assessment of the latter feature is often carried out, in most of the studies dealing with vector-valued *IMs*, assessing the reduction of record-to-record variability of structural response via the least squares methods. An alternate attracting option, more directly linked to seismic reliability assessment of structures, is to evaluate the *IMs* with respect to estimation of failure

* Corresponding author. Tel./fax: +52 667 7134053.
E-mail address: ebojorq@uas.uasnet.mx (E. Bojórquez).

0141-0296/$ - see front matter © 2012 Elsevier Ltd. All rights reserved.
http://dx.doi.org/10.1016/j.engstruct.2012.07.002

probability, that is, seismic fragility. This can give direct insights on the comparative efficiency of the considered intensity with respect to the chosen response measures.

The need to assess which ground motion intensity measure is more capable of predicting the probability of failure of a structure with accuracy in the case of narrow-band motions, motivated the study presented in this paper. Seismic fragility analyses, computed by means of several vector-valued *IMs*, for steel framed structures subjected to the records from the soft-soil of Mexico City, were compared referring to both peak and cyclic structural response measures. This, as discussed in the following, may provide insights on the efficiency of the *IMs*, in particular that of the *secondary* parameter of the vector, and on how much it is helpful to include it in the assessment along the *primary IM*.

In fact, all the vector-valued *IMs* here considered are based on $Sa(T_1)$ as the first parameter. As the second component of the vector, *PGA*, *PGV*, ground motion duration (t_D) established according to Trifunac and Brady [17] as the time interval delimited by the instants of time at which the 5% and 95% of the Arias Intensity occurs, the I_D factor proposed by Cosenza and Manfredi [18], the parameter $R_{T1,T2}$ [8], and the parameter N_p [12], were alternatively used.

It is important to underline that the choice of selecting vectors where the first component is always *Sa* follows two main reasons. (1) As mentioned above, current hazard maps in many countries are mostly based on this parameter. Because any structural risk assessment requires hazard available, it is especially worth to consider intensity measures based on *Sa*. In fact, it has been proven that if hazard is available for *Sa*, then the hazard for the other parameter may be easily obtained conditionally (e.g., [19]). In other words, the study attempts to investigate, comparatively, advanced intensity measures for which hazard may be derived by that for *Sa*. (2) Beside the hazard availability, several studies discuss the advantages and disadvantages of using *Sa* (e.g., [20]). On the other hand, some of the limitations of *Sa* (e.g., inability to capture energy demand) are believed to be possibly solved by vector-valued *IMs*, but few, if any, comparative studies are available in literature (e.g., [12]). In this sense, the study by the authors is part of current efforts trying to capture the best parameter directly related with structural response looking at the seismic fragility, which is the final result of structural assessment to be integrated with hazard to obtain seismic risk.

The vector-valued *IMs* were selected to account for maximum and cumulative damage potential of ground motion. Seismic fragility is evaluated considering two different structural response parameters: (i) the maximum inter-story drift which is the most common peak-response parameter in the seismic design codes to control the structural behavior, and (ii) a recently proposed energy-based damage index for steel frames related to cyclic-response [21,22].

The presentation is organized so that vector-valued *IMs*, the structural models, the selected earthquake ground motion records, and the performance parameters are described first. Then, the procedure to perform seismic fragility analysis of the steel frames under narrow-band motions, and the results are shown. Next, a discussion of which *IM* is found (and why) with the best explicative power to estimate the probability of failure of steel frames under narrow-band earthquake ground motions, is given. Finally, an empirical correlation study for the *IMs* and the structural response measures considered, is addressed.

2. Methodology

2.1. Vector-valued IMs

Of the six different vector-valued ground motion *IMs* considered, the first two, $\langle Sa(T_1), PGA\rangle$ and $\langle Sa(T_1), PGV\rangle$, are expected to be especially linked to peak structural response by means of both components of the vectors. The second pair of *IMs*, $\langle Sa(T_1), t_D\rangle$ and $\langle Sa(T_1), I_D\rangle$, was selected to represent a combination of peak and cumulative damage potential of ground motion (hence accounting, in the latter case, for the influence of ground motion duration). I_D is defined as in Eq. (1), where $a(t)$ is the acceleration time-history and t_E is the total duration of the record.

$$I_D = \frac{\int_0^{t_E} a(t)^2 dt}{PGA \cdot PGV} \quad (1)$$

The last two *IMs* considered are $\langle Sa(T_1), R_{T1,T2}\rangle$ and $\langle Sa(T_1), N_p\rangle$. These carry information about the spectral shape, which has been recently elected as the principal ground motion feature expressing the earthquake potential, especially for structures following modern seismic design principles. $R_{T1,T2}$ is the ratio of the spectral acceleration at period T_2 divided by spectral acceleration at period T_1, where T_2 is a period larger than T_1; N_p is defined in Eq. (2), where $Sa_{avg}(T_1,\ldots,T_N)$ represents the geometrical mean between the periods T_1 and T_N [12].

$$N_p = \frac{Sa_{avg}(T_1,\ldots,T_N)}{Sa(T_1)} \quad (2)$$

N_p was developed to take into account the informative potential of the elastic response spectrum at periods beyond the fundamental one. In fact, if one or a set of n records feature a mean N_p value close to one, it may be expected the average spectrum to be about flat between T_1 and T_N. For a value of N_p lower than one, it is expected an average spectrum with negative slope beyond T_1. In the case of N_p values larger than one, the spectra tend to increase beyond T_1.

In this study, T_2 equal to twice the first mode period was chosen, consistent with other studies [8,23,24]. Also Bojórquez and Iervolino [12] observed that the value of T_N around 2 or 2.5 times T_1 is adequate in most of the cases.

It is recalled that the normalization of the geometrical mean with respect to the spectral acceleration at the fundamental period, lets N_p be independent with respect to the scaling level. Moreover, seismic hazard analysis for this *IM* alone, can be performed with already available tools.

2.2. Structural models and ground motion records

Four regular steel frames designed according to the Mexico City Seismic Design Provisions [25] were considered. The frames, which were assumed to be for office occupancy, have three bays of 8 m and a number of stories from 4 to 10, with a story height of 3.5 m (see Fig. 1). The frames were designed for ductile behavior. A36 steel and W-shape sections were used for the beams and columns of the frames. An elastic–plastic model with 3% strain-hardening was considered to model the cyclic behavior of the steel members [26]. The critical damping ratio was assumed equal to 3%.

Relevant characteristics for each frame, such as the fundamental period of vibration (T_1), the seismic coefficient and roof displacement at yielding (C_y and D_y, respectively) are shown in Table 1 (the latter two were evaluated from pushover analysis).

The frames have been selected because Meli and Avila [27] found that most of the damages in Mexico City due to the 1985 Earthquake were recorded in buildings with structural periods from 0.5 to 1.5 s, which are smaller than that of the soil (about two seconds).

The case study structures were subjected to thirty narrow-band, soft-soil, and long duration ground motions, which were recorded in the Lake Zone of Mexico City during seismic events with magnitudes near of seven or larger, on soil having a dominant period of two seconds according to [25]. The records were taken from the Mexican Strong Motion Database [28], and their main characteristics are

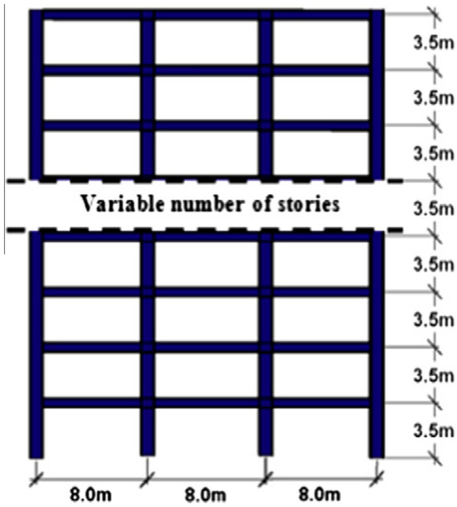

Fig. 1. Geometrical characteristics of the steel frames.

Table 1
Structural properties of steel frames under consideration.

Frame	Number of stories	T_1 (s)	C_y	D_y (m)
F4	4	0.90	0.45	0.136
F6	6	1.07	0.42	0.174
F8	8	1.20	0.38	0.192
F10	10	1.37	0.36	0.226

summarized in Table 2. The response spectra of the records scaled for similar values of $Sa(T_1)$ at a period of T = 0.90 s are illustrated in Fig. 2.

2.3. Structural performance parameters

The seismic fragility of the selected structures (to follow) is obtained by expressing structural response in terms of maximum inter-story drift (*MIDR*) and an energy based damage index, I_{DEN}, as engineering demand parameters (*EDPs*). The capacity in terms of *MIDR* used corresponds to 0.03, which is the maximum inter-story drift capacity of steel frames according to [25]. (Furthermore, this inter-story drift limit was selected because Bojórquez et al. [22] found that 0.03 may be considered acceptable for models which account for cumulating earthquake damage.)

A measure of damage in terms of normalized plastic hysteretic energy can be formulated as in Eq. (3) [21], where I_{DEN} characterizes damage in terms of normalized plastic hysteretic energy; and E_{ND} and E_{NC} represent the demand and capacity of the structure in such a way that I_{DEN} equal to one implies the structural failure.

$$I_{DEN} = \frac{E_{ND}}{E_{NC}} \tag{3}$$

In Eq. (3), while E_{ND} for a particular frame is estimated as the sum of the plastic hysteretic energy dissipated by all its structural members, E_{NC} can be estimated following the recommendation given by Akbas [29] and Bojórquez et al. [30] as:

$$E_{NC} = \frac{\sum_{i=1}^{N_S} (2 \cdot N_B \cdot Z_f \cdot F_y \cdot \theta_{pa} \cdot F_{EHi})}{C_y \cdot D_y \cdot W} \tag{4}$$

where N_S and N_B are the number of stories and bays in the building, respectively; F_{EHi}, an energy participation factor that accounts for the different contribution of each story to the energy dissipation capacity of the frame (see also [30]); Z_f, the section modulus of the flanges of the elements; F_y, the yield stress; and θ_{pa}, the cumulative plastic rotation capacity of the structural steel elements; and W is the total weight of the structure. This equation considers that the plastic energy is dissipated exclusively through plastic behavior at both ends of the beams of the frames. A θ_{pa} = 0.23 was used to characterize the normalized plastic hysteretic energy capacity at the ends of the beams [22]. Note that this damage measure is expected to be related to cyclic structural response and therefore to ground motion duration [30–34].

3. Analyses and results

The numerical results of the seismic fragility analyses, by means of the different vector-valued ground motion *IMs*, are presented in this section. Fragility assessment was developed via incremental dynamic analysis (IDA) [3]. To this aim, the frames were subjected to the narrow-band records at different intensities by means of amplitude scaling[1] of the first component, $Sa(T_1)$, of the vector-valued *IMs*, and then applying logistic regression to fit failure (F) and non-failure cases, for the second parameter.

When the seismic demand is larger than the capacity in terms of a specific *EDP*, the value of probability of failure is equal to one, while it is zero otherwise. In fact, the structural performance of a structure subjected to a record is associated to the realization of a Bernullian random variable according to which 1 represents failure, and 0 represents non-failure. In such cases, logistic regression is an appropriate way to find dependency of failure on the *dose* of a continuous variable, as the investigated *IMs* are. Although logistic regression analyses were developed for a range of spectral accelerations via multinomial logistic regression, yielding to fragility surfaces (to follow), to derive information about efficiency of the secondary intensity measures, results for a fixed spectral acceleration are shown first. In fact, in this case fragility curves are obtained, which are easier to be analyzed visually.

3.1. Fragility curves

Fragility curves, given a specific $Sa(T_1)$ value (x_1), are obtained applying logistic regression to failure and non-failure cases as a function of the second parameter of the vector. In fact, in this case, the probability of failure, P_F, is obtained as:

$$P_F = P[F|S_a(T_1) = x_1, IM_2 = x_2] = \frac{1}{1 + e^{(-\beta_1 - \beta_2 \cdot x_2)}} \tag{5}$$

where IM_2 is the secondary parameter of the vector, while β_1 and β_2 are coefficients obtained from regression of the results for the records scaled at $Sa(T_1) = x_1$. Scaling the records at the same *Sa*, in fact, allows to compare the explicative power, with respect to the structural response measures considered, of the secondary components of the vector-valued *IMs*. In this sense the resulting fragility curves are the failure probabilities conditional on the specific $Sa(T_1)$ value, Eq. (5).

Given the primary parameter of the vector-valued *IMs*, the efficiency of the secondary one may be measured by how flat the fragility curves are. Steep curves indicate significant explanatory power of the second component of the vector[2]; conversely, flat

[1] The peculiar features of the ground motions considered in the study call into question the use of scaling for IDA when significant soil nonlinearity may occur that will affect the properties of high-Sa ground motions significantly relative to those of low-Sa motions. This could, in principle, impair classical scaling procedure (e.g., [3,7,13]). However, to address relevance of this issue is not straightforward and beyond the primary scope of the work. The reader is referred to the work of Bazzurro and Cornell ([35] and [36]) for a discussion of the role of nonlinear site effects in the performance-based earthquake engineering context.

[2] This visual inspection of fragility curves is often appropriate as numerical goodness of fit measures for logistic regression are difficult to address; see Iervolino and Cornell [37] for a discussion on this same issue.

Table 2
Earthquake ground motion basic information.

Record	Date	Earthquake	Moment magnitude	Epicentral distance (km)	Station	PGA (cm/s^2)	PGV (cm/s)	t_D (s)	I_D
1	19/09/1985	Michoacán	8.1	366	SCT	178.0	59.5	34.8	15.5
2	21/09/1985	Michoacán	7.6	323	Tlahuac deportivo	48.7	14.6	39.9	19.9
3	25/04/1989	Guerrero	6.9	293	Alameda	45.0	15.6	37.8	17.8
4	25/04/1989	Guerrero	6.9	294	Garibaldi	68.0	21.5	65.5	11.1
5	25/04/1989	Guerrero	6.9	289	SCT	44.9	12.8	65.8	17.3
6	25/04/1989	Guerrero	6.9	286	Sector Popular	45.1	15.3	79.4	28.1
7	25/04/1989	Guerrero	6.9	295	Tlatelolco TL08	52.9	17.3	56.6	11.1
8	25/04/1989	Guerrero	6.9	293	Tlatelolco TL55	49.5	17.3	50.0	14.0
9	14/09/1995	Oaxaca-Guerrero	7.3	303	Alameda	39.3	12.2	53.7	17.3
10	14/09/1995	Oaxaca-Guerrero	7.3	303	Garibaldi	39.1	10.6	86.8	34.7
11	14/09/1995	Oaxaca-Guerrero	7.3	286	Liconsa	30.1	9.62	60.0	14.5
12	14/09/1995	Oaxaca-Guerrero	7.3	298	Plutarco Elías Calles	33.5	9.37	77.8	33.8
13	14/09/1995	Oaxaca-Guerrero	7.3	295	Sector Popular	34.3	12.5	101.2	30.8
14	14/09/1995	Oaxaca-Guerrero	7.3	304	Tlatelolco TL08	27.5	7.8	85.9	30.0
15	14/09/1995	Oaxaca-Guerrero	7.3	303	Tlatelolco TL55	27.2	7.4	68.3	21.3
16	09/10/1995	Colima	7.5	536	Cibeles	14.4	4.6	85.5	29.4
17	09/10/1995	Colima	7.5	537	CU Juárez	15.8	5.1	97.6	36.6
18	09/10/1995	Colima	7.5	537	Centro urbano Presidente Juárez	15.7	4.8	82.6	34.9
19	09/10/1995	Colima	7.5	537	Córdoba	24.9	8.6	105.1	26.5
20	09/10/1995	Colima	7.5	537	Liverpool	17.6	6.3	104.5	29.4
21	09/10/1995	Colima	7.5	539	Plutarco Elías Calles	19.2	7.9	137.5	40.8
22	09/10/1995	Colima	7.5	540	Sector Popular	13.7	5.3	98.4	27.4
23	09/10/1995	Colima	7.5	541	Valle Gómez	17.9	7.18	62.3	21.9
24	11/01/1997	Michoacán	6.9	379	CU Juárez	16.2	5.9	61.1	22.6
25	11/01/1997	Michoacán	6.9	379	Centro urbano Presidente Juárez	16.3	5.5	85.7	25.2
26	11/01/1997	Michoacán	6.9	381	García Campillo	18.7	6.9	57.0	21.4
27	11/01/1997	Michoacán	6.9	381	Plutarco Elías Calles	22.2	8.6	76.7	27.7
28	11/01/1997	Michoacán	6.9	380	Est. # 10 Roma A	21.0	7.76	74.1	29.8
29	11/01/1997	Michoacán	6.9	380	Est. # 11 Roma B	20.4	7.1	81.6	24.3
30	11/01/1997	Michoacán	6.9	383	Tlatelolco TL08	16.0	7.2	57.5	19.9

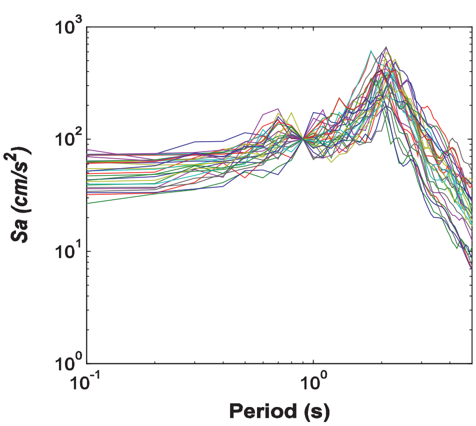

Fig. 2. Elastic response spectra for the records scaled at the same spectral ordinate $S_a(T_1)$ = 100 cm/s^2 for T = 0.9s and 3% of critical damping.

trends mean that the *IM* on the abscissa does not add information to failure prediction.

The fragilities when *MIDR* is considered as an *EDP*, are illustrated in Fig. 3 for $Sa(T_1)$ = 1000 cm/s^2 and the frame F4. As expected, *PGA* and *PGV* seem not to be very explicative given spectral acceleration as the logistic curve is relatively flat, which means that a significant change in the *IM* does not lead to an important change in failure probability.

In the case of t_D and I_D, although they are expected to be more related to cyclic structural response (because they are believed to be measures of the cumulative damage potential of the ground motion), fragilities in terms of *MIDR* are steeper with respect to those in terms of *PGA* and *PGV*. t_D appears to be of some significance to predict the probability of failure in terms of *MIDR*. This seems, at a glance, in contradiction with respect to Iervolino et al. [31] and Bojórquez et al. [38]; however in the cited studies records had durations much lower with respect to those considered herein.

The *IMs* based on the spectral shape, $R_{T1,T2}$ and N_p, result in the addition of significant information to fragility, given $Sa(T_1)$. This has been shown before [8,9,37], when maximum inter-story drift is the *EDP*. Based on the cases addressed in this study, it is observed that N_p results in one of the more informative parameter with respect to fragility in a similar manner, if not slightly more, with respect to the other *IMs*. This may be related to the fact that N_p includes the spectral ordinates in a range, while $R_{T1,T2}$ uses, as a proxy for the spectral shape, the values at the end of an interval. However, for this same reason, the latter is easier to handle with respect to the former, but the former provides more information about the spectral shape, which is crucial at least in the case of narrow-band motions as those considered here [12].

Fig. 4 shows the probability of failure in terms of the energy-based damage index (or the cyclic structural demand) for all the selected *IMs* and frame F10. In this case, note that the fitted curves are almost horizontal for *PGA* and *PGV*, indicating a negligible relationship between these parameters and the failure probability when it is based on energy demand in structures, given $Sa(T_1)$. For t_D and I_D the results are still very similar to those obtained for *MIDR*, but in the case of I_D there is a little improvement in the prediction of the probability of failure for the cyclic structural response if compared to *MIDR*, as expected [31]. On the other hand, $R_{T1,T2}$ and N_p are, again, those *IMs* that are best related to the probability of failure based on cyclic structural response. In fact, the logistic regression for N_p illustrates how well it represents the structural response, as the curve is steeper than all other parameters.

Conclusions hold for fragilities of structures not shown in the figures. In fact, Tables 3 and 4 compare the β coefficients obtained from the logistic regression for all the frames and both engineering demand parameters under consideration.

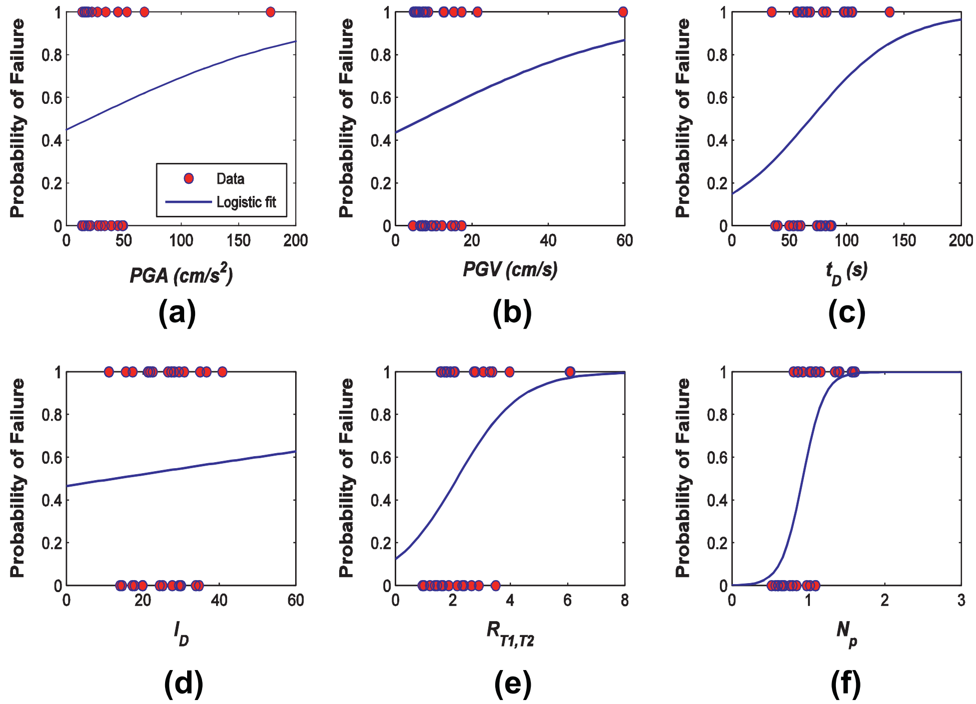

Fig. 3. Comparing probability of failure in terms of *MIDR* using logistic regression for frame F4 at $Sa(T_1) = 1000$ cm/s^2 versus: (a) *PGA*; (b) *PGV*; (c) t_D; (d) I_D; (e) $R_{T1,T2}$; and (f) N_p.

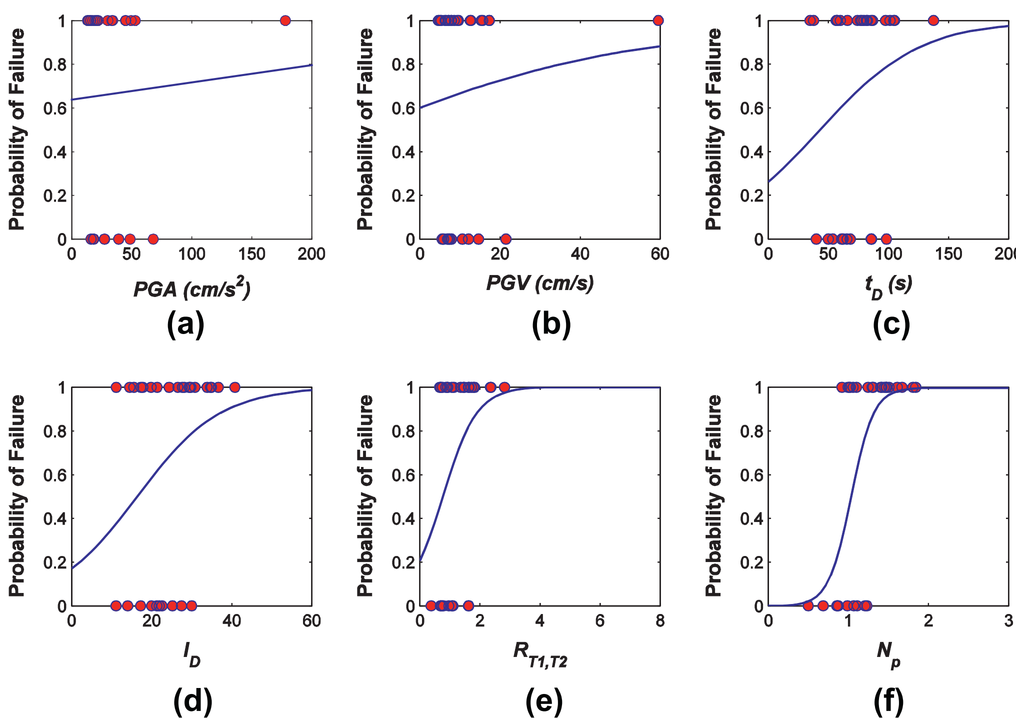

Fig. 4. Comparing probability of failure in terms of I_{DEN} using logistic regression for frame F10 at $Sa(T_1) = 1000$ cm/s^2 versus: (a) *PGA*; (b) *PGV*; (c) t_D; (d) I_D; (e) $R_{T1,T2}$; and (f) N_p.

3.2. Fragility surfaces via multiple logistic regression

The previous section had shown in a simple way, for one $Sa(T_1)$ level, that if the fragility curves tend to be horizontal, the selected secondary *IM* is of poor significance with respect to structural failure, and on the other hand, if the curves are steep, the parameter under consideration adds information to failure probability. Nevertheless, the discussion previously developed was only valid for a specific level of intensity in terms of $Sa(T_1)$. To generalize the results, in this section multiple logistic regression is applied, using both parameters of the vector, via the following equation:

$$P_F = P[F|S_a(T_1) = x_1, IM_2 = x_2] = \frac{1}{1 + e^{(-\beta_1 - \beta_2 \cdot x_1 - \beta_3 \cdot x_2)}} \quad (6)$$

Table 3
Values of the β coefficients for the logistic regression in terms of *MIDR* at $Sa(T_1)$ = 1000 cm/s^2.

Frame	*PGA*		*PGV*		t_D		I_D		$R_{T1,T2}$		N_p	
	β_1	β_2	β_1	β_2	β_1	β_2	β_1	β_2	β_1	β_2	β_1	β_2
F4	−0.204	0.010	−0.258	0.036	−1.75	0.026	−0.135	0.011	−1.954	0.912	−6.70	7.20
F6	−0.267	0.012	−0.246	0.035	−1.941	0.028	−0.443	0.024	−5.331	1.738	−8.18	4.67
F8	0.0002	0.013	−0.239	0.062	−3.114	0.049	−0.808	0.050	−1.330	0.766	−17.1	10.93
F10	−1.190	0.024	−1.670	0.119	−1.688	0.017	−0.779	0.015	−2.771	1.85	−11.5	8.78

Table 4
Values of the β coefficients for the logistic regression in terms of I_{DEN} at $Sa(T_1)$ = 1000 cm/s^2.

Frame	*PGA*		*PGV*		t_D		I_D		$R_{T1,T2}$		N_p	
	β_1	β_2	β_1	β_2	β_1	β_2	β_1	β_2	β_1	β_2	β_1	β_2
F4	0.521	0.001	0.406	0.013	−2.080	0.037	−0.558	0.046	−4.794	2.635	−27.02	32.19
F6	0.449	0.003	0.476	0.006	−1.556	0.029	−1.237	0.075	−5.794	2.152	−9.808	6.019
F8	1.479	0.004	1.461	0.014	−2.893	0.069	−0.848	0.109	−1.426	1.546	−8.427	6.976
F10	0.565	0.004	0.410	0.026	−1.036	0.024	−1.578	0.096	−1.335	1.758	−7.364	7.123

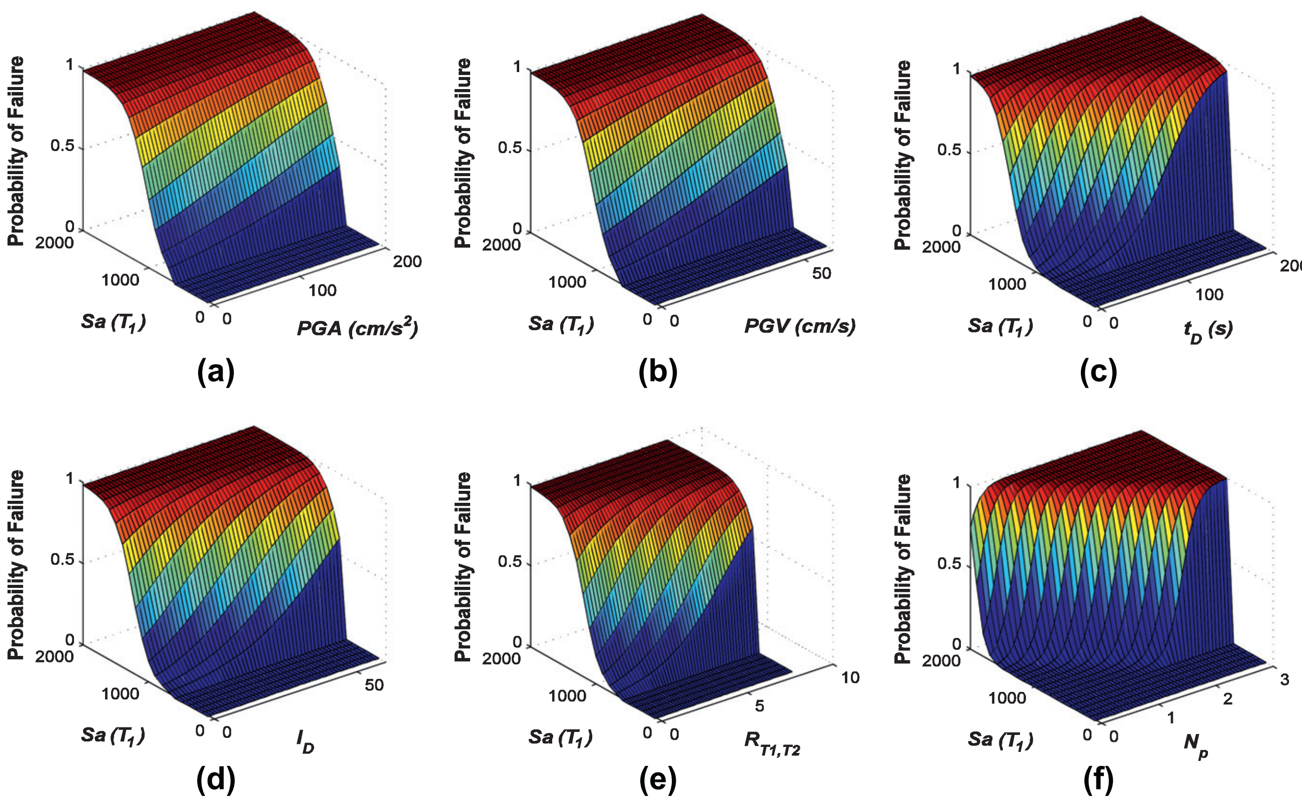

Fig. 5. Probability of failure in terms of *MIDR* for frame F8 versus $Sa(T_1)$ and (a) *PGA*; (b) *PGV*; (c) t_D; (d) I_D; (e) $R_{T1,T2}$; and (f) N_p.

where β_1, β_2 and β_3 are obtained from regression analysis of the results including variation of both *IMs*. In this way fragility surfaces as a function of the vector-valued *IMs* are obtained.

Multiple logistic regressions are shown in Fig. 5 for frame F8 in the case of *MIDR* as an *EDP*. In Fig. 6 the results for the energy-based damage index are depicted for frame F6. It seems confirmed that for the whole range of spectral acceleration considered, the vector of *IMs* with the more explicative power with respect to fragility is $\langle Sa(T_1), N_p\rangle$.

The results of multiple logistic regression also support the conclusion that vector-valued *IMs* based on a combination of parameters related with peak ground motion are not especially helpful with respect to scalar *IMs*. In fact, for example in the case of *PGA* and *PGV*, the curvature of the surfaces in directions of these *IMs* is negligible, indicating that only $Sa(T_1)$ affects fragility. Conversely, curvature of the surfaces where N_p and other more informative parameters are included, is far from cylindrical. Conclusions hold for those structural cases not shown in these two figures.

To further understand the results, the following section compares the correlation among all the selected *IMs* and the *EDPs*. Furthermore, the correlations between $Sa(T_1)$ and the six parameters considered as the second component of the vectors, are also estimated.

3.3. Correlation of vector-valued IMs with MIDR and I_{DEN}

The dependence of structural fragility with the ground motion intensity measures can be further illustrated if the coefficient of correlation between the selected vector-valued intensity measures

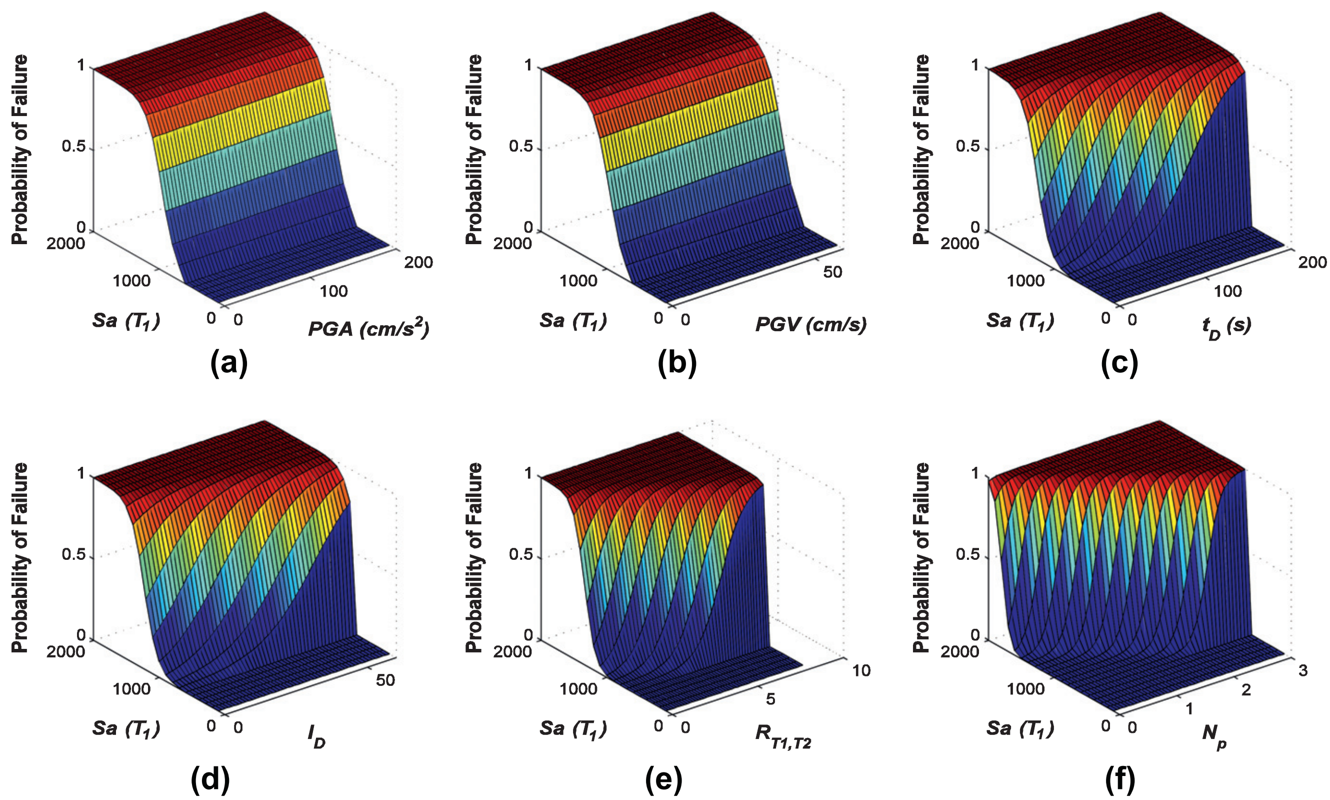

Fig. 6. Probability of failure in terms of I_{DEN} for frame F6 versus $Sa(T_1)$ and (a) *PGA*; (b) *PGV*; (c) t_D; (d) I_D; (e) $R_{T1,T2}$; and (f) N_p.

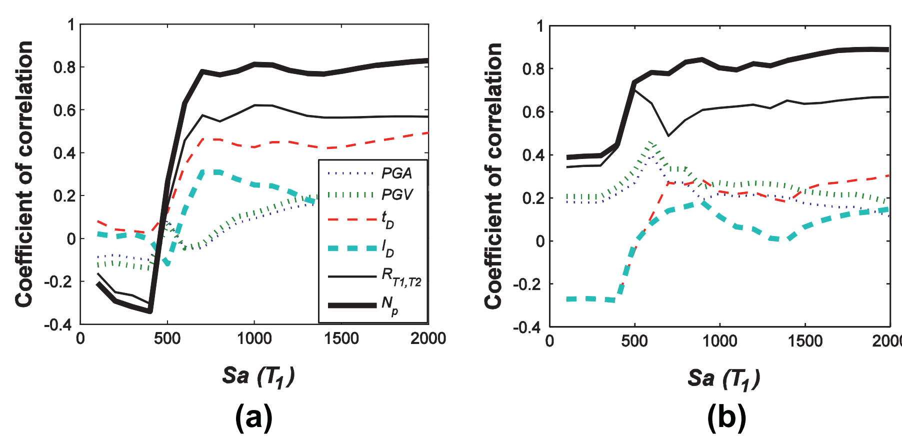

Fig. 7. Correlation among the six vector-valued *IMs* with *MIDR* for frame F4 and F10.

and the engineering demand parameters under consideration is analyzed. If the coefficient of correlation is larger for some specific *IM*, then it can be concluded that it is a *better* parameter to estimate the structural response. The coefficients of correlation have been estimated for all the frames, and using the six *IMs* and both *EDPs* selected, for each scaling level of spectral acceleration.

The results of the coefficients of correlation of the vector-valued *IMs* and the *MIDR* for frames F4 and F10 are illustrated in Fig. 7. As it was observed in the estimation of fragility, the maximum values of the coefficients of correlations are observed when the vector $\langle Sa(T_1), N_p\rangle$ is selected as intensity measure. Note that the correlation coefficient is low for small values of spectral acceleration, since in this case the standard deviation of the structural response is also small because of the linear behavior of the structure.

Similar results are observed for the case of frames F6 and F8 in Fig. 8, which provides the correlation among the *IMs* and the energy-based damage index. This figure suggests that there is a clear relation between I_{DEN} with $\langle Sa(T_1), N_p\rangle$. The curves in Fig. 8 begin at *Sa* equal to 500 cm/s^2, because for smaller values the hysteretic energy dissipated is zero (i.e., elastic structural response).

It can be observed, in general, that spectral-shape-based *IMs* are more correlated with the structural response to narrow-band earthquake ground motions. These conclusions hold for those structural cases not shown in the figures.

3.4. Correlation of primary and secondary IMs in the vectors

One way to better understand the results presented above of fragility and correlation among the *IMs* with the structural

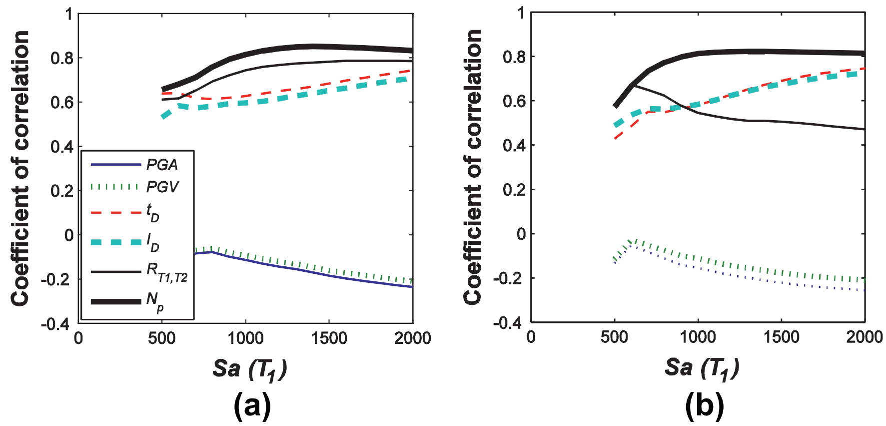

Fig. 8. Correlation among the six vector-valued *IMs* with I_{DEN} for frame F6 and F8.

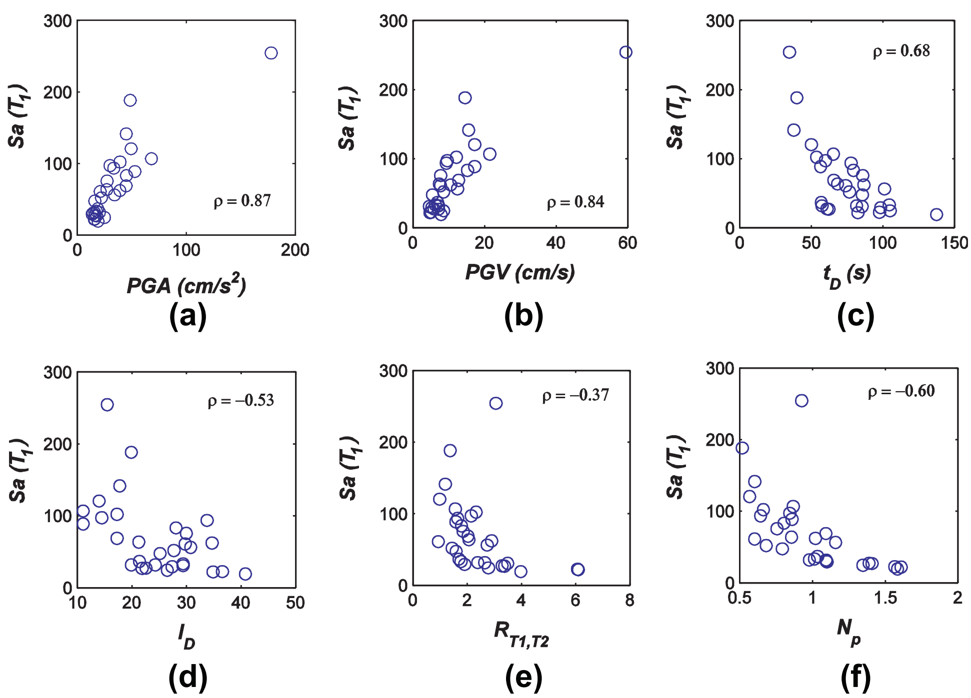

Fig. 9. Comparison of the relation between $Sa(T_1)$ versus (a) *PGA*; (b) *PGV*; (c) t_D; (d) I_D; (e) $R_{T1,T2}$; and (f) N_p.

response may be by comparing the scatter plots in Fig. 9a and b, where the relationships of *PGA* and *PGV* with $Sa(T_1)$ for $T_1 = 0.9$ s (the structural period of frame F4), are given for the considered ground motions.

The figures show a strong linear relationship between *PGA* and *PGV* with respect to the spectral acceleration (coefficient of correlation, ρ, close to 0.9), which means that adding *PGA* does not factually add information with respect to $Sa(T_1)$. (In fact, if the correlation coefficient was equal to one it would mean that there was a deterministic linear relationship between $Sa(T_1)$ and *PGA* (or *PGV*), indicating that one parameter is only a variable transformation of the other; i.e., it does not give additional information of the ground motion.)

Panels c–f of Fig. 9 illustrate less correlation between the other secondary parameters with the spectral acceleration at the first mode of vibration, indicating how these give information not included in $Sa(T_1)$.

4. Conclusions

The evaluation of probability of failure of steel frames subjected to narrow-band ground motions from Mexico City (Mexico) was estimated employing six vector-valued ground motion intensity measures and peak and cumulative seismic response measures.

Among the *IMs*, two are based on a combination of peak parameters of ground motion $\langle Sa(T_1), PGA\rangle$ and $\langle Sa(T_1), PGV\rangle$; two are based on peak and cumulative damage potential parameters $\langle Sa(T_1), t_D\rangle$ and $\langle Sa(T_1), I_D\rangle$; and two are based on the spectral shape $\langle Sa(T_1), R_{T1,T2}\rangle$ and $\langle Sa(T_1), N_p\rangle$.

The comparisons of the results, indicate that for steel frames under narrow-band motions, adding another peak ground motion parameter to $Sa(T_1)$ is generally not worthwhile, regardless of the structural response measure considered. Conversely, the vectors which include measures of the spectral shape appear to be the most efficient in estimating probability of failure.

It was generally observed that $\langle Sa(T_1), N_p\rangle$ is the most representative parameter, for both maximum inter-story drift and cyclic structural demand, among the *IMs* compared herein.

Note that, although these conclusions are based on structures subjected to narrow-band motions, it is expected that for other type of records results may be similar. This is because emerging vector-valued *IMs* (i.e., N_p, and spectral-shape-based intensity measures in general) appear able to capture structural response information contained in any spectral shape and, therefore, seem promising for other types of ground motion.

As a side result, it was found the significance of $\langle Sa(T_1), t_D\rangle$ independently if peak displacement or energy-based response parameters are considered. The latter was expected, while the influence of duration on *MIDR* response was less anticipated. This is believed to be mostly related to the very long duration of records considered herein with respect to most of the literature on the topic.

Acknowledgements

The support given by El Consejo Nacional de Ciencia y Tecnología CONACYT, La Universidad Autónoma de Sinaloa under Grant PROFAPI 2011/029 and DGAPA (PAPIIT)-UNAM is appreciated. Authors want to thank the anonymous reviewers for their comments, which improved quality and readability of the paper. Finally, Racquel K. Hagen of Stanford University is also gratefully acknowledged for proofreading the paper.

References

[1] Cornell CA, Krawinkler H. Progress and challenges in seismic performance assessment. PEER Center News 2000;3(2).
[2] Deierlein GG. Overview of a comprehensive framework for performance earthquake assessment. Report PEER 2004/05. Pacific Earthquake Engineering Center; 2004. p. 15–26.
[3] Vamvatsikos D, Cornell CA. Incremental dynamic analysis. Earthq Eng Struct Dynam 2002;31(3):491–514.
[4] Housner GW. Spectrum intensities of strong motion earthquakes. In: Proceedings of the symposium on earthquake and blast effects on structures. Earthquake Engineering Research Institute; 1952.
[5] Arias A. A measure of earthquake intensity. In: Hansen RJ, editor. Seismic design for nuclear power plants. Cambridge (MA): MIT Press; 1970. p. 438–83.
[6] Von-Thun JL, Rochin LH, Scott GA, Wilson JA. Earthquake ground motions for design and analysis of dams. In: Earthquake engineering and soil dynamics: II. Recent advance in ground-motion evaluation. Geotechnical special publication 20. New York: ASCE; 1988. p. 463–81.
[7] Shome N. Probabilistic seismic demand analysis of nonlinear structures. PhD thesis, Stanford University; 1999.
[8] Cordova PP, Dierlein GG, Mehanny SSF, Cornell CA. Development of a two parameter seismic intensity measure and probabilistic assessment procedure. The second U.S.-Japan workshop on performance-based earthquake engineering methodology for reinforce concrete building structures, Sapporo, Hokkaido; 2001. p. 187–206.
[9] Baker JW, Cornell CA. A vector-valued ground motion intensity measure consisting of spectral acceleration and epsilon. Earthq Eng Struct Dynam 2005;34:1193–217.
[10] Riddell R. On ground motion intensity indices. Earthq Spectra 2007;23(1):147–73.
[11] Yakut A, Yilmaz H. Correlation of deformation demands with ground motion intensity. J Struct Eng – ASCE 2008;134(12):1818–28.
[12] Bojórquez E, Iervolino I. Spectral shape proxies and nonlinear structural response. Soil Dynam. Earthq. Eng. 2001;31(7):996–1008.
[13] Iervolino I, Cornell CA. Records selection for nonlinear seismic analysis of structures. Earthq. Spectra 2005;21(3):685–713.
[14] Bazzurro P, Cornell CA. Vector-valued probabilistic seismic hazard analysis. In: 7th U.S. national conference on earthquake engineering, earthquake engineering research institute, Boston, MA; 2002.
[15] Elefante L, Jalayer F, Iervolino I, Manfredi G. Disaggregation-based record selection and modification for seismic risk assessment of structures. Soil Dynam. Earthq. Eng. 2010;30(12):1513–27.
[16] Buratti N. Confronto tra le performance di diverse misure di intensità dello scuotimento sísmico. *XIV Convegno Nazionale "L'Ingegneria Sismica in Italia"*. ANDIS Bari; 2011 [in Italian].
[17] Trifunac MD, Brady AG. A study of the duration of strong earthquake ground motion. Bull Seismol Soc Am 1975;65(3):581–626.
[18] Cosenza E, Manfredi G. The improvement of the seismic-resistant design for existing and new structures using damage criteria. In: Fajfar P, Krawinkler H, editors. Seismic design methodologies for the next generation of codes. Rotterdam: Balkema; 1997. p. 119–30.
[19] Iervolino I, Giorgio M, Galasso C, Manfredi G. Conditional hazard maps for secondary intensity measures. Bull Seismol Soc Am 2010;100(6):3312–9.
[20] Luco N. Probabilistic seismic demand analysis, SMRF connection fractures, and near-source effects. PhD thesis. Stanford University; 2002.
[21] Bojórquez E, Reyes-Salazar A, Terán-Gilmore A, Ruiz SE. Energy-based damage index for steel structures. Steel Compos Struct 2010;10(4):343–60.
[22] Bojórquez E, Terán-Gilmore A, Ruiz SE, Reyes-Salazar A. Evaluation of structural reliability of steel frames: inter-story drifts versus plastic hysteretic energy. Earthq Spectra 2011;27(3):661–82.
[23] Baker JW. Vector-valued ground motion intensity measures for probabilistic seismic demand analysis. PhD thesis, Stanford University; 2005.
[24] Bojórquez E, Iervolino I, Manfredi G. Evaluating a new proxy for spectral shape to be used as an intensity measure. In: 2008 Seismic engineering international conference commemorating the 1908 Messina and Reggio Calabria, Earthquake (MERCEA'08); 2008.
[25] Mexico City Seismic Design Provisions. Normas Técnicas Complementarias para el Diseño por Sismo. Departamento del Distrito Federal; 2004 (in Spanish).
[26] Bojórquez E, Rivera JL. Effects of degrading models for ductility and dissipated hysteretic energy in uniform annual failure rate spectra. In: The 14th world conference on earthquake engineering, Beijing, China; 2008.
[27] Meli R, Avila JA. The Mexico earthquake of September 19, 1985 analysis of building response. Earthq Spectra 1989;5(1):1–18.
[28] Alcántara L, Quass R, Pérez C, Ayala M, Macías M, Sandoval H, et al. Base Mexicana de Datos de Sismos Fuertes, CD-ROM edited by Sociedad Mexicana de Ingeniería Sísmica, vol. 2; 2000.
[29] Akbas B. Energy-based earthquake resistant design of steel moment resisting frames. PhD thesis, Department of Civil and Architectural Engineering, Illinois Institute of Technology; 1997.
[30] Bojórquez E, Ruiz SE, Terán-Gilmore A. Reliability-based evaluation of steel structures using energy concepts. Eng Struct 2008;30(6):1745–59.
[31] Iervolino I, Manfredi G, Cosenza E. Ground motion duration effects on nonlinear seismic response. Earthq Eng Struct Dynam 2006;35:21–38.
[32] Hancock J, Bommer JJ. A state-of-knowledge review of the influence of strong-motion duration on structural damage. Earthq Spectra 2006;22(3):827–45.
[33] Terán-Gilmore A, Jirsa JO. Energy demands for seismic design against low cycle fatigue. Earthq Eng Struct Dynam 2007;36:383–404.
[34] Rodríguez ME, Padilla C. A damage index for the seismic analysis of reinforced concrete members. J Earthq Eng 2008;13(3):364–83.
[35] Bazzurro P, Cornell CA. Ground-motion amplification in nonlinear soil sites with uncertain properties. Bull Seismol Soc Am 2004;94(6):2090–109.
[36] Bazzurro P, Cornell CA. Nonlinear soil-site effects in probabilistic seismic-hazard analysis. Bull Seismol Soc Am 2004;94(6):2110–23.
[37] Iervolino I, Cornell CA. Probability of occurrence of velocity pulses in near-source ground motions. Bull Seismol Soc Am 2008;98(2):2262–77.
[38] Bojórquez E, Iervolino I, Manfredi G, Cosenza E. Influence of ground motion duration on degrading SDOF systems. In: 1st European conference on earthquake engineering and seismology, Geneva (Switzerland), 3–8 September 2006 [paper # 425].